

Crystal and Molecular Structures of New Chromone Derivatives as Empirical Evidence of Intramolecular Proton Transfer Reaction; Ab Initio Studies on Intramolecular H-Bonds in Enaminones

Agnieszka J. Rybarczyk-Pirek,[†] Sławomir J. Grabowski,^{*,†,‡} Magdalena Małecka,[†] and Jolanta Nawrot-Modranka[§]

Department of Crystallography and Crystallochemistry, University of Łódź, ul. Pomorska 149/153, 90-236 Łódź, Poland, Institute of Chemistry, University of Białystok, Al. J. Piłsudskiego 11, 15-443 Białystok, Poland, and Laboratory of Bioinorganic Chemistry, Faculty of Pharmacy, Medical University, ul. Muszyńskiego 1, Łódź, Poland

Received: June 5, 2002; In Final Form: October 4, 2002

The crystal and molecular structures of two new phosphorochromones determined by single-crystal X-ray diffraction are presented. The existence of two tautomers stabilized by intramolecular N–H···O and O–H···N hydrogen bonds and environmental effects in crystals is observed as evidence of the proton transfer reaction. The proton transfer process within simple enaminones being analogues of the compounds studied by X-ray diffraction methods is investigated using MP2/6-311++G** and MP4/6-311++G** levels of theory. The Bader theory is also applied in the analysis of the hydrogen bonding within investigated systems. The results indicate that the systems with N–H···O intramolecular hydrogen bonds are more stable than those containing O–H···N bonds.

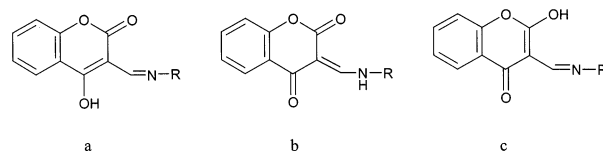
Introduction

Chromone analogues are widely known for their various biological activities and pharmacological properties.^{1–4} On the other side, phosphoramides and phosphorohydrazides were found to exhibit anticancer activity^{5–8} by alkylating nucleophilic centers of nucleobases and amino acids. Modification of a phosphorohydrazide molecule containing a heterocyclic system gives the possibility of designing and synthesizing novel compounds of interesting properties. Thus, many chromone derivatives with a phosphonic acid substituent have been synthesized.^{9,10} They are of our interest because of their alkylation properties in vitro in the Preussmann test with 4-(4'-nitrobenzyl)pyridine (NBP)¹¹ and their expected antitumor activity in vivo. Obviously, this anticipated application requires a detailed knowledge and additional pharmacological tests on further properties such as the ability to cross biological membranes, toxicity, and stability in biological media.

There is still little known about phosphorohydrazide derivatives of chromone and their potential biological activity; the possible application in cancer chemotherapy makes the knowledge of their molecular structure of great importance. Hence, in continuation of our previous research on this group of compounds,^{12–14} the crystal structures of (*E*)-3-[[[(diphenoxyphosphoryl)-2-methylhydrazine]methylene]-4-hydroxy-2*H*-1-benzopyran-2-one (**1**) and 3-[[[(diphenoxythio-phosphoryl)hydrazine]methylidene]-3,4-dihydro-2*H*-1-benzopyran-2,4-dione (**2**) have been determined by X-ray diffraction method and are analyzed here.

Compounds **1** and **2** may exist in three tautomeric forms (Scheme 1). Therefore, the aim of this study is not only to get

SCHEME 1: Possible Tautomers of Investigated Compounds^a



^a R: –N(CH₃)–P(O)(OC₆H₅)₂– for **1** (a form); –NH–P(S)(OC₆H₅)₂– for **2** (b form).

insight into the crystal and molecular structures of **1** and **2** but also to obtain information about their stable tautomers. The tautomeric forms of 4-hydroxycoumarine were observed and described in earlier studies,¹⁵ but the substitution of the hydrazone moiety in position 3 of the heterocyclic ring gives the possibility of existence of a new tautomeric form, b (Scheme 1). For the molecules of investigated compounds, each form is additionally stabilized by a NH···O or OH···N intramolecular hydrogen bond.

The crystallographic results clearly indicate two different tautomeric forms; enol (a) and enamine (b) for **1** and **2** structures, respectively. On the basis of these results, the data from the Cambridge Structural Database¹⁶ that searched for related compounds involving pyrane system have been analyzed and compared.

It should be mentioned that two tautomeric forms a and b found in crystal structures may be treated as two different stages of the intramolecular proton transfer process. The similar tautomeric forms were described for O–H···O hydrogen bonds in π -conjugated systems.¹⁷ For a better understanding of the process of the intramolecular proton transfer, the part of this study has been focused on ab initio calculations. Such calculations for simple enaminones have been performed to analyze the influence of the substituents on the existence of different tautomeric forms. Additionally, the atoms-in-molecules (AIM)

* To whom correspondence should be addressed. E-mail: slagra@krysia.uni.lodz.pl.

[†] University of Łódź.

[‡] University of Białystok.

[§] Medical University.

TABLE 1: Crystallographic Data and Structure Refinement

	1	2
formula	C ₂₃ H ₁₉ N ₂ O ₆ P	C ₂₂ H ₁₇ N ₂ O ₅ PS
<i>M</i>	450.37	452.41
crystal system	monoclinic	triclinic
space group	<i>P</i> 2 ₁ / <i>n</i>	<i>P</i> 1̄
<i>a</i> (Å)	8.304(1)	11.031(1)
<i>b</i> (Å)	10.396(1)	13.317(1)
<i>c</i> (Å)	24.695(3)	7.405(1)
α (deg)		100.38(1)
β (deg)	99.46(1)	95.38(1)
γ (deg)		99.80(1)
<i>V</i> (Å ³)	2101.9(4)	1045.7(1)
<i>Z</i>	4	2
<i>D_x</i> (g cm ⁻³)	1.423	1.437
<i>μ</i> (mm ⁻¹)	1.546	2.430
<i>T</i> (K)	293(2)	293(2)
λ (Å)	1.54178	1.54178
index ranges	-10 ≤ <i>h</i> ≤ 10; 0 ≤ <i>k</i> ≤ 13; 0 ≤ <i>l</i> ≤ 31	-10 ≤ <i>h</i> ≤ 13; -16 ≤ <i>k</i> ≤ 16; -8 ≤ <i>l</i> ≤ 8
no. of data collected	4332	4197
no. of unique data	4235	3983
<i>R</i> _{int}	0.0182	0.0226
no. of <i>I</i> > 2σ(<i>I</i>) data	3020	2639
no. of parameters	366	349
<i>R</i> ₁ (all data) ^a	0.0619	0.0702
<i>wR</i> ₂ (all data) ^b	0.1141 ^d	0.1183 ^c
<i>R</i> ₁ [<i>I</i> > 2σ(<i>I</i>)] ^a	0.0354	0.0410
<i>wR</i> ₂ [<i>I</i> > 2σ(<i>I</i>)] ^b	0.1040 ^d	0.1120 ^c
Δρ _{min} (e Å ⁻³)	-0.245	-0.300
Δρ _{max} (e Å ⁻³)	0.200	0.205

^a $R_1 = \sum(|F_o - F_c|)/\sum|F_o|$. ^b $wR_2 = [\sum w(|F_o - F_c|)^2/\sum|F_o|^2]^{1/2}$. ^c $w = \exp(1.2 \sin^2\theta/\lambda)/[\sigma^2(F_o^2) + (0.059P)^2]$. ^d $w = 1/[\sigma^2(F_o^2) + (0.033P)^2 + 0.950P]$ where $P = [(F_o^2) + 2(F_c^2)]/3$.

theory of Bader¹⁸ has been applied to examine geometrical and topological parameters of the studied systems.

Methods

Experimental. *Compound 1.* Equimolar amounts of methyl 4-oxo-4*H*-1-benzopyran-3-carboxylate (0.8 g) and N¹-diphenoxythiophosphoro-N¹-methylhydrazid (1.0 g) were solved in 10 cm³ of anhydrous methanol and refluxed for 2 h. After it was cooled, the product was precipitated and recrystallized from methanol. A 1.36 g (83%) amount of compound **1** (mp 157–159 °C) was obtained. IR (KBr) $\nu_{\max}/\text{cm}^{-1}$: 3600–3300 (OH), 1710 (C=O), 1635 (C=N), 1275 (P=O), 1210–1180 (POAr). ¹H NMR (CDCl₃): δ_H 3.26 (d, *J*_{P-CH₃} = 7.98 Hz, 3H, CH₃), 7.14–8.06 (m, 14H, arom), 8.08 (s, 1H, -CH=N), 13.73 (s, broad, 1H, OH). ³¹P NMR (CDCl₃): δ_P -6.07.

Compound 2 was obtained and described earlier.¹⁰

The melting point is uncorrected. The IR spectrum was taken on a Pye-Unicam 200 G spectrometer. The ¹H NMR spectrum at 100 MHz was recorded on a Tesla BS 567A, and ³¹P NMR was recorded on a Bruker HX360 spectrometer with H₃PO₄ as external standard.

Transparent, colorless crystals of both compounds suitable for X-ray diffraction were obtained after recrystallization from methanol by slow evaporation of the solvent at room temperature. Single crystals were mounted on glass fibers. Data were collected at room temperature on a Rigaku AFC5S diffractometer¹⁹ for **1** and on a Kuma KM4 diffractometer²⁰ for **2**, using Cu Kα X-ray source and a graphite monochromator. The unit cell dimensions were determined from a least-squares fit to setting angles of set reflections—25 for **1** and 95 for **2**, respectively. Intensities of three standard reflections measured after each group of 150 reflections showed no significant decays

TABLE 2: Selected Bond Lengths (Å) and Angles (deg)

	1	2
P(1)–O(2)/S(2)	1.450(2)	1.893(1)
P(1)–O(11)	1.574(2)	1.595(2)
P(1)–O(21)	1.586(2)	1.581(2)
P(1)–N(3)	1.645(2)	1.653(2)
N(3)–N(4)	1.382(2)	1.405(3)
N(4)–C(5)	1.284(3)	1.306(3)
C(5)–C(63)	1.454(3)	1.389(3)
C(62)–O(621)	1.206(3)	1.213(3)
C(64)–O(641)	1.335(3)	1.247(3)
O(61)–C(62)	1.374(3)	1.376(3)
O(61)–C(69)	1.379(3)	1.387(3)
C(62)–C(63)	1.448(3)	1.442(3)
C(63)–C(64)	1.365(3)	1.433(3)
C(64)–C(70)	1.440(3)	1.464(3)
C(69)–C(70)	1.387(3)	1.384(4)
O(2)/S(2)–P(1)–O(11)	117.2(1)	118.0(1)
O(2)/S(2)–P(1)–O(21)	116.2(1)	118.8(1)
O(2)/S(2)–P(1)–N(3)	113.0(1)	113.6(1)
O(11)–P(1)–N(3)	103.4(1)	107.4(1)
O(21)–P(1)–N(3)	105.8(1)	99.5(1)
O(11)–P(1)–O(21)	99.4(1)	97.5(1)
P(1)–N(3)–N(4)	115.5(2)	117.8(2)
N(3)–N(4)–C(5)	119.8(2)	120.5(2)
N(4)–C(5)–C(63)	118.8(2)	123.2(2)
C(5)–C(63)–C(62)	116.5(2)	116.6(2)
C(5)–C(63)–C(64)	122.4(2)	121.2(2)
C(62)–C(63)–C(64)	120.2(2)	122.1(2)
O(61)–C(62)–C(63)	118.1(2)	118.0(2)
O(61)–C(62)–O(621)	116.7(2)	115.5(2)
O(63)–C(62)–O(621)	125.2(2)	126.4(2)
C(69)–O(61)–C(62)	121.7(2)	121.6(2)
C(63)–C(64)–O(641)	122.4(2)	122.3(2)
C(70)–C(64)–O(641)	116.9(2)	121.5(2)
C(63)–C(64)–C(70)	120.7(2)	116.2(2)
C(63)–C(5)–N(4)–N(3)	177.1(2)	-175.5(2)
C(5)–N(4)–N(3)–P(1)	-178.8(2)	89.5(3)
C(5)–N(4)–N(3)–C(31)/H(31)	3.8(3)	-89(2)
N(4)–N(3)–P(1)–O(2)/S(2)	170.0(1)	179.2(2)

under X-ray irradiation. All data were corrected for Lorentz and polarization factors. Absorption corrections were applied.^{21,22}

The method of refinement for both compounds was the same. The structures were solved by direct methods using SHELXS-86²³ and refined by full-matrix least-squares method on *F*² using SHELXL97.²⁴ After the refinement with isotropic displacement parameters, refinement was continued with anisotropic displacement parameters for all nonhydrogen atoms. Positions of hydrogen atoms were found on a difference Fourier map and refined. In the final step of the refinement procedure, all nonhydrogen atoms were refined with anisotropic thermal displacement parameters and hydrogen atoms with isotropic thermal displacement parameters, respectively. A summary of crystallographic relevant data is given in Table 1.

The molecular geometry was calculated by PARST97²⁵ and PLATON.²⁶ Selected bond distances and angles of **1** and **2** are summarized in Table 2. The drawings were made by PLATON. Further experimental details, coordinates, and displacement parameters are in Supporting Information.

Computational Details. All of the calculations of this study were performed using the Gaussian 94²⁷ and Gaussian 98²⁸ series of programs. The geometry optimizations were carried out at the MP2/6-311++G** level of theory.²⁹ The use of diffuse functions seems to be justified since it is the proper approach for studies of H-bonded systems.³⁰ The enol and keto forms of simple enaminones are considered here, and the transition states (TS) for these tautomeric forms are taken into account (Scheme 2). The two simplest tautomeric forms, iminoenol and enaminon (with R₁=R₂=R₃=R₄=H), and their

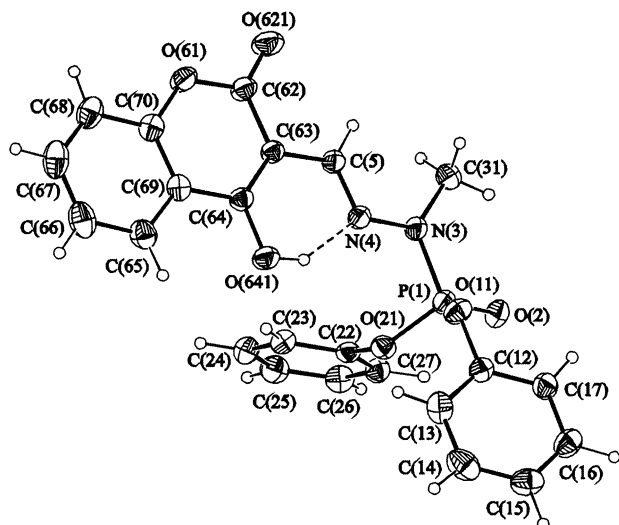
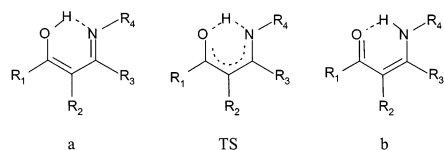
SCHEME 2: Tautomeric Forms (a and b) and the TS of the Calculated Systems


Figure 1. Molecular structure of **1** with atom labeling scheme. The displacement ellipsoids are drawn at the 30% probability level.

TS are optimized not only at the MP2/6-311++G** but also at the MP4/6-311++G** level of theory. The remaining calculations for derivatives where $R_1=F$, $R_3=F$ and for $R_4=Li$ have been performed at the MP2/6-311++G** level.

The AIM theory of Bader¹⁸ is also applied in this study to localize the positions of the bond critical points (BCPs) and the ring critical points (RCPs). The properties of BCPs and RCPs may be a very useful tool in the analysis of interatomic linkages such as covalent bonds and contacts. Among the contacts, the hydrogen bonds are the most often investigated.^{31,32} The electronic densities at critical points and their Laplacians are analyzed here.

Results and Discussion

Crystallographic Studies. The molecular structures of **1** and **2** as observed in crystals are presented in Figures 1 and 2. A summary of crystallographic data is given in Table 1. The selected molecular geometry parameters are given in Table 2.

The difference between molecules of **1** and **2** concerns the phosphorhydrazide substituent, while the coumarine fragments are the same. The condensed ring systems are planar with the maximum deviation from corresponding least-squares plane of 0.037(3) Å for C(63) and 0.032(3) Å for C(67), for **1** and **2**, respectively. As expected, the benzenoid rings are flat within experimental errors.

For the crystal structure of **2**, N–H bonds (those connected with the P atom) act as proton donors within N–H···O intermolecular hydrogen bonds; O(621) atoms are accepting centers for such H-bonds. There is no such interaction for structure **1** since there are NCH₃ groups in **1** instead of N–H bonds. Hence, for the crystal structure **2**, there is an infinite chain of molecules situated along the *c*-axis. This chain may be designated as C(5) according to the graph set theory notation.³³ The resulting pattern is shown in Figure 3. Table 3 presents the geometrical parameters of intramolecular H-bonds

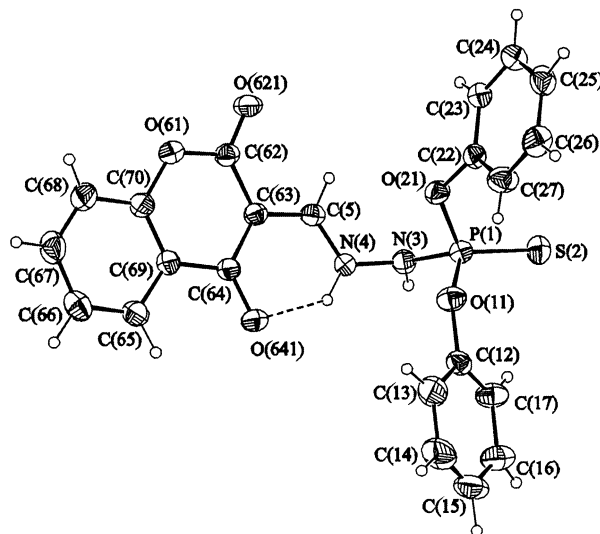


Figure 2. Molecular structure of **2** with atom labeling scheme. The displacement ellipsoids are drawn at the 30% probability level.

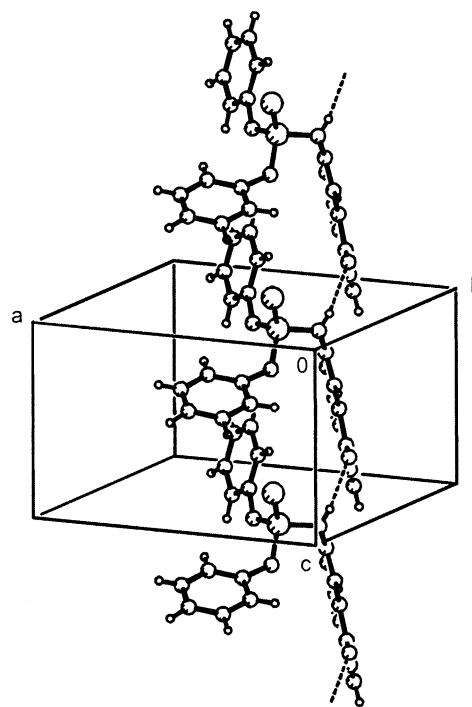


Figure 3. Chains of molecules linked by N–H···O hydrogen bonds (dotted lines) in the crystal structure of **2**.

TABLE 3: Hydrogen-Bonding Geometry (Å, deg)

	D–H	H···A	D···A	D–H···A	graph set descriptor
1					
O(641)–H(41)···N(4) ^b	0.89(3)	1.79(3)	2.586(3)	146(3)	S(6)
2					
N(4)–H(41)···O(641) ^b	0.91(3)	1.88(3)	2.609(3)	135(2)	S(6)
N(3)–H(31)···O(621) ^{a,c}	0.76(4)	2.15(4)	2.899(3)	166(3)	C(5)

^a *x*, *y*, *z* + 1. ^b Intramolecular H-bonds. ^c Intermolecular H-bond.

of **1** and **2** structures and of intermolecular H-bond existing for structure **2**. We see that the H···N distance for the O–H···N bridge is shorter than H···O for N–H···O suggesting that the first type of intramolecular H-bond is slightly stronger than the second one. The mentioned above contacts are equal to 1.79 and 1.88 Å, respectively. The described above intermolecular H-bonds of crystal structure **2** not only influence the arrangement

of molecules in the crystal but also induce changes within molecular structure. For example, the N(3)–P(1)–O(2) group is much closer to coplanarity with the coumarine moiety for **1** (dihedral angle $15.4(1)^\circ$) than the N(3)–P(1)–S(2) group for **2** ($88.7(1)^\circ$). The situation of the N–P–O(S) group toward the coumarine fragment influences the resonance effect within the corresponding fragments of molecules; as a consequence, we may observe different lengths of the N(4)–N(3) bond within **1** and **2**, 1.382 and 1.405 Å, respectively. We see that the kind of substituent at the N atom influences not only the molecular conformation well-characterized by differences in C(5)–N(4)–N(3)–P(1) torsion angles (Table 2) but also the other geometrical parameters of molecules such as bond lengths and angles. The kind of substitution at the N atom also influences the existence of additional intermolecular N–H \cdots O bonds as for the crystal structure **2** and consequently the arrangement of molecules (Figure 3).

Although we observe an enol form for the molecular structure **1** and an enamine form for **2**, an essential and common structural feature for both structures is an intramolecular hydrogen-bonding interaction. It is the reason that we observe the planarity of the corresponding parts of molecules and the resonance effects within C(64)–C(5)–N(4)–N(3) fragments. The resulting hydrogen-bonding pattern is the same in both compounds (six-membered ring involving one donor and one acceptor atom), and the existence of different tautomeric forms leads to equalization of selected bonds in comparison with the corresponding standard values.³⁴

Tautomeric forms a and c (Scheme 1) may be considered as hydroxyl derivatives of coumarine and chromone, respectively. The search of the Cambridge Crystallographic Database has revealed 11 4-hydroxycoumarine derivatives and no 2-hydroxychromone derivatives except for two compounds with partially saturated heterocyclic rings. This finding is in agreement with the other studies on the stability of coumarine tautomers¹⁵ and indicates that a is usually a more stable form for the species existing in the crystal structures.

On the other side, taking into consideration tautomeric forms a and b and considering only the heterocyclic ring of aromatic character, 13 structures corresponding to b with N–H \cdots O intramolecular hydrogen bonds and two structures corresponding to a were found. However, no O–H \cdots N bonds within the investigated systems were observed. We may conclude that the OH \cdots N interaction in **1** is the first case of such an intramolecular hydrogen bond in pyrane derivatives observed in the crystal structure.

Ab Initio and AIM Results. A series of molecules related to malonaldehyde, containing an intramolecular H-bond, were analyzed using different ab initio and density functional theory (DFT) techniques^{35,36} of calculations as well as topological approaches as the Bader theory.^{37,38} For example, simple derivatives of malonaldehyde were studied in terms of ab initio and AIM calculations.³⁹ Proton transfer within the intramolecular H-bond between N atoms in excited electronic states of 1,5-diaza-1,3-pentadiene was also studied.⁴⁰ The studies on the intramolecular H-bond in thiomalonaldehyde (TMA) were performed using ab initio, DFT, and AIM approaches;³⁸ the relative stabilities of the HBs in TMA and its tienol tautomer using high-level ab initio calculations were analyzed, and substituent effects on the strength of H-bonds were also studied.³⁷

It has been pointed out that for the crystal structures of enaminones there are intramolecular N–H \cdots O hydrogen bonds, which should be assisted by resonance.⁴¹ The similar resonance-assisted hydrogen bonds (RAHBs) should exist for their

tautomers (Scheme 2). However, for the solid state, one of the tautomeric forms, b (Schemes 1 and 2), is more common. Different RAHBs were found within crystal structures, among them the systems related to enaminones, but tautomeric form a was not reported.⁴¹ The similar result may be observed if one searches the Cambridge Structural Database. However, for the crystal structures of enaminones analyzed in this study, both a and b tautomeric forms are observed. For **1**, we observe the intramolecular O–H \cdots N hydrogen bond while for **2** the more common tautomeric form is stabilizing by the N–H \cdots O hydrogen bond. If we take into account the H–O–C(R₁)=C(R₂)–C(R₃)=N–R₄ intramolecular ring for **1** or the O=C(R₁)–C(R₂)=C(R₃)–N(R₄)–H ring for **2**, we may say about two stages of the proton transfer reaction. The only difference within structures analyzed here, except for the mentioned above intramolecular ring, is for the R₄ substituent, which is N(CH₃)–P(O)(OC₆H₅)₂ for **1** and NH–P(S)(OC₆H₅)₂ for **2**. It may suggest that the nature of the R₄ substituent influences which of the tautomeric forms is more stable in the crystal. It is also in line with the well-known statement of Bürgi and Dunitz^{42,43} that each of the crystal structures may be treated as a frozen state corresponding to the particular stage of the reaction. According to this approach, the crystal structures reported here (**1** and **2**) correspond to two stages of the reaction of the proton transfer: N \cdots H–O \rightleftharpoons N–H \cdots O. It has been pointed out earlier that there is a sufficient number of precise neutron diffraction results to represent the reaction path for the process of the proton transfer for –C=O \cdots H–O–C \rightleftharpoons C–O–H \cdots O=C– systems⁴⁴ or to study the proton transfer process from the neutral to zwitterionic forms of amino acids.⁴⁵

The ab initio calculations were performed in this study on simple enaminones to get insight into the process of the proton transfer for this class of compounds. Table 4 shows the geometrical parameters for these intramolecular H-bonded systems optimized within the MP2/6-311++G** level of theory. We see that R₁–R₄ are usually H atoms substituted for some systems by F atoms. Additionally, the system with R₄=Li is considered in this study. Tautomeric form a corresponds to the O–H \cdots N hydrogen bond (Scheme 2) while tautomeric form b is that one corresponding to the N–H \cdots O H-bond. Table 4 also presents the geometrical parameters of the TSs. For the simplest system where all R substituents are H atoms, the additional calculations for both a and b tautomeric forms and for the TS were performed at the MP4/6-311++G** level of theory (Table 4).

There are the following regular findings concerning the geometrical parameters presented in Table 4. The results suggest that the H-bonds of the TSs are the strongest ones since the N \cdots O distances are the shortest for them in comparison with the corresponding tautomeric forms a and b. For all studied systems, the N \cdots O distances for TS are shorter than 2.4 Å. The other geometrical data support it since the H \cdots O and H \cdots N contacts are also shortest for TSs and the N–H–O angles of the corresponding H-bonds are the closest to linearity. The same geometrical parameters, H \cdots O, H \cdots N, and N \cdots O distances and H-bond angles, indicate that O–H \cdots N bonds are stronger than the corresponding N–H \cdots O bonds. Table 4 also shows the electron delocalization within the intramolecular H-bonded ring. For RAHBs, for example, for those that are the derivatives of malonaldehyde, the delocalization is reflected by the equalization of C=C, C–C and C=O, C–O bonds.^{17,39} For the systems investigated here, there are no corresponding pairs of C–N, C=N and C=O, C–O bonds within the same systems. Hence, the delocalization is represented by the difference between C–C and C=C bond lengths (Table 4). We can see that the greatest

TABLE 4: Geometrical Parameters (Å, deg) of Both Tautomeric Forms and of TS for the Systems Analyzed Here

R ₁ , R ₂ , R ₃ , R ₄	tautomeric form	d(O,H)	d(H,N)	d(O,N)	<(O,H,N)	R _{C=C} -R _{C=C}	energy (hartree)
H, H, H, H	a	1.002	1.675	2.580	148.0	0.077	-246.6634153
	TS	1.190	1.269	2.390	152.7	0.024	-246.6593244
H, H, H, H	b	1.957	1.015	2.705	128.2	0.070	-246.6727647
	a ^a	0.984	1.779	2.650	145.5	0.099	-246.6918453
F, H, H, H	TS ^a	1.200	1.258	2.387	152.4	0.029	-246.6836332
	b ^a	2.023	1.012	2.744	126.2	0.084	-246.7013529
H, H, F, H	b	2.058	1.012	2.765	125.0	0.070	-345.7807103
	a	0.992	1.752	2.635	146.2	0.078	-345.7572490
H, H, H, F	TS	1.247	1.221	2.397	152.3	0.006	-345.7490944
	b	1.914	1.018	2.682	129.7	0.072	-345.7573292
H, H, H, F	a	0.980	1.831	2.668	141.3	0.088	-345.6722600
	TS	1.356	1.141	2.367	142.8	0	-345.6534211
H, H, H, Li	b	1.948	1.016	2.591	118.5	0.062	-345.6582375
	b	1.938	1.027	2.813	141.3	0.036	-253.5642892

^a MP4 results.**TABLE 5: Topological Parameters (in au) of Both Tautomeric Forms and of TS for the Systems Analyzed Here**

R ₁ , R ₂ , R ₃ , R ₄	tautomeric form	$\rho_{O,H}$	$\rho_{H,N}$	$\nabla^2\rho_{O,H}$	$\nabla^2\rho_{H,N}$	ρ_{RCP}	$\nabla^2\rho_{RCP}$
H, H, H, H	a	0.3153	0.0564	-2.175	0.117	0.0194	0.127
	TS	0.1817	0.1589	-0.379	-0.863	0.0245	0.171
	b	0.0276	0.3287	0.102	-1.825	0.0147	0.092
H, H, H, H	a ^a	0.3365	0.0436	-2.392	0.115	0.0173	0.112
	TS ^a	0.1764	0.1639	-0.331	-0.261	0.0240	0.171
	b ^a	0.0239	0.3349	0.092	-1.811	0.0135	0.085
F, H, H, H	b	0.0219	0.3322	0.084	-1.812	0.0138	0.083
	a	0.3256	0.0467	-2.288	0.113	0.0186	0.117
	TS	0.1559	0.1797	-0.140	-0.390	0.0247	0.172
H, H, H, F	b	0.0304	0.3228	0.108	-1.819	0.0153	0.097
	a	0.3394	0.0370	-2.413	0.108	0.0163	0.101
	TS	0.1173	0.2225	0.083	-0.086	0.0230	0.160
H, H, H, Li	b	0.0293	0.3270	0.112	-1.975	0.0158	0.098
	b	0.0292	0.3234	0.100	-1.561	0.0157	0.093

^a From MP4 wave function.

is the delocalization for TSs, next to systems with N-H...O bonds, and the lowest delocalization is for molecules with O-H...N bonds. It is in line with experimental results presented here. For the structure **1** with an O-H...N hydrogen bond, the difference between the CC bond lengths within the resonance intramolecular system amounts to 0.075 Å while this difference for the structure **2** with a N-H...O hydrogen bond is equal to 0.044 Å.

Table 4 presents the energies (in hartrees) of the systems. Generally, the molecules with the intramolecular N-H...O bonds are more stable than the corresponding systems with O-H...N bonds. As mentioned above, it may be supported by the number of the corresponding crystal structures found in the Cambridge Structural Database. It is in agreement with the previous X-ray diffraction results on similar structures to those investigated here; it was pointed out that the formation of structures with strong intramolecular N-H...O hydrogen bonds assisted by resonance is favored.⁴¹

For the molecules with R_i = H (i = 1-4), the tautomeric form b is more stable than a (Table 4); the difference in energy between tautomeric forms amounts to 5.9 and 6.0 kcal/mol for MP2/6-311++G** and MP4/6-311++G** levels of theory, respectively. For R₃=F, there is no practical difference between both tautomers. For R₁=F and for the system with R₄=Li, there are no tautomers of the type a, i.e., with O-H...N bonds; for both cases, the structures a collapse without activation barrier to structures b. These results may explain why for the crystal structure **1** the tautomeric form a exists while for the crystal structure **2** the tautomeric form b exists. For these structures, there are differences for substituents attached to the nitrogen atom. We see from the calculations on modeled systems that

for R₄=Li the only existing form is b and for R₄=F the tautomeric form a is more stable.

Table 5 shows the topological parameters of the systems investigated here. There are electron densities at OH and NH BCPs as well as at H...N and H...O BCPs. Table 5 also gives the values of the RCPs since all systems are characterized by the presence of the intramolecular H-bonds.

The RCP is a point of the minimum electron density within the ring surface and a maximum on the ring line.¹⁸ For example, in the case of benzene, the RCP lies in the center of the ring owing to symmetry constraints. In the absence of symmetry, an RCP can be found anywhere inside the ring. In this paper, RCPs existing for intramolecular H-bonds are considered.

The values of Laplacians for all electron densities of BCPs and RCPs are also given. We see a well-known tendency that the electron density for BCP of a covalent bond is greater than the electron density of the contact for the H-bond within the same system. Additionally, if two tautomeric forms (a and b) exist, the electron density at the H...N contact of tautomer a is greater than this value for the H...O of tautomer b. It is in line with the suggestion given above that O-H...N bonds are stronger than N-H...O ones. It was pointed out in the previous literature⁴⁶⁻⁴⁸ that the electron density at H...Y BCP (Y represents the proton acceptor center within hydrogen bridge) correlates well with H-bond energy, especially for homogeneous samples.⁴⁹ Table 5 also shows that $\rho_{H...Y(N \text{ or } O)}$ is the greatest for TSs. Figure 4 presents the correlation between H...Y (O or N) distance and $\rho_{H...Y(N \text{ or } O)}$; both values may be treated as descriptors of H-bond strength.^{49,50} We can see a good correlation between these descriptors although different kinds of contacts are taken into account.

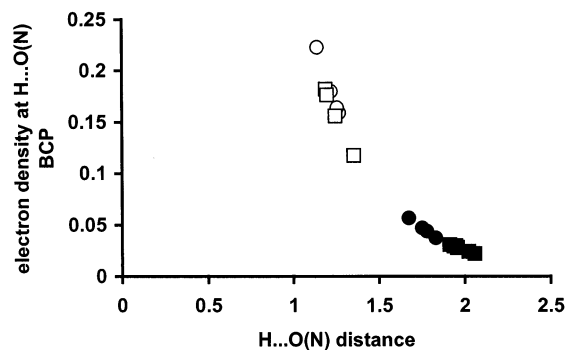


Figure 4. Correlation between the H \cdots Y distance (Y, the proton-accepting center: O or N) and the electron density at the H \cdots Y BCP; full circles represent H \cdots N contacts, full squares represent H \cdots O bonds, and open circles and squares correspond to the same values of the TSs.

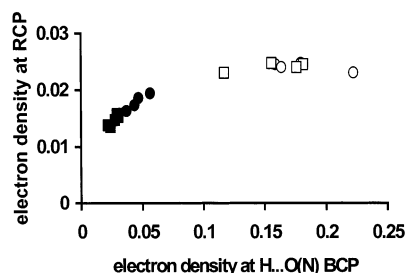


Figure 5. Correlation between the electron density at H \cdots Y BCP and the electron density at the RCP of the ring created due to the formation of an intramolecular H-bond; the designations of this figure correspond to those of Figure 4.

Recent investigations show that the properties of RCPs may be treated as descriptors of H-bond strength for intramolecular H-bonds.⁵¹ The correlation between electron density at H \cdots Y BCP within an H-bonded system and the electron density at RCP is present at Figure 5. There is also a lot of other topological evidences of the existence of the H-bond.⁵² Among them, there is the elongation of the radius of hydrogen toward the proton-accepting center. Such property is nicely shown within the contour maps of tautomeric forms a, b and the TS for the system with R₃=F (Figure 6). We see that the H atom radius is shorter toward the X atom (X–H is the proton-donating bond) and longer toward the Y (Y designates the proton-accepting center). Figure 6c representing the contour map of the TS shows the equalization of H atom radii in both mentioned above directions. The similar equalization for the other TS considered in this study (for R substituents being H atoms) shows the molecular graph presented in Figure 7.

Conclusions

Two crystal structures with intramolecular H-bonds are analyzed here showing the existence of N–H \cdots O and O–H \cdots N interactions. Such H-bonds may be treated as two stages of the proton transfer reaction. The search through the Cambridge Structural Database shows that the structures with N–H \cdots O bonds are more common than the structures with O–H \cdots N bonds.

The ab initio calculations at MP2/6-311++G** and MP4/6-311++G** levels of theory confirm the findings mentioned above. For all simple derivatives of enaminones considered in this study, the tautomeric forms with N–H \cdots O bonds exist. The other tautomeric forms with O–H \cdots N bonds are usually less stable or collapse into the second tautomeric form during the calculations. The energies of the systems also show that forms with N–H \cdots O bonds are more stable. The analysis of

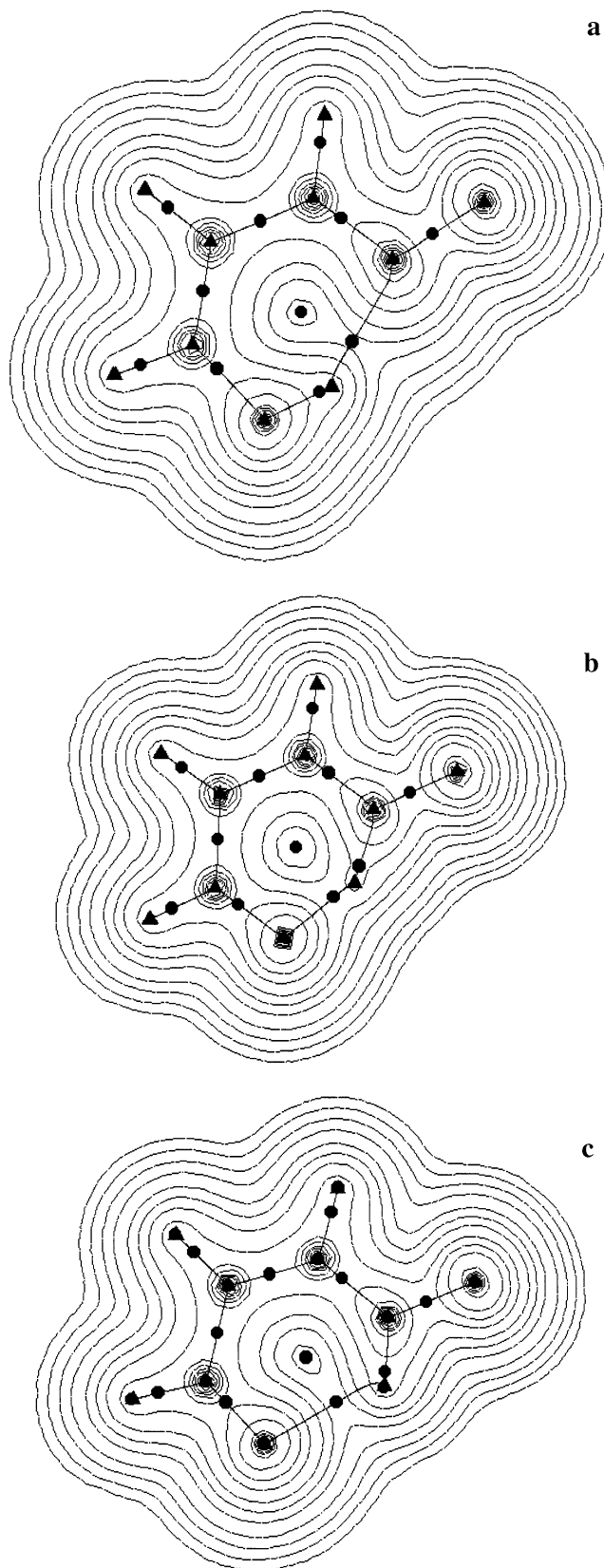


Figure 6. Contour maps of two tautomeric forms (a and c) and of the TS (b) for one of the systems investigated here; triangles correspond to attractors while circles correspond to BCPs and RCPs.

the computational results obtained within ab initio and AIM methods shows that O–H \cdots N hydrogen bonds are stronger than N–H \cdots O ones although for the whole systems those are less stable, which contain O–H \cdots N bridges. The results of ab initio calculations also show that the type of the substituent at the

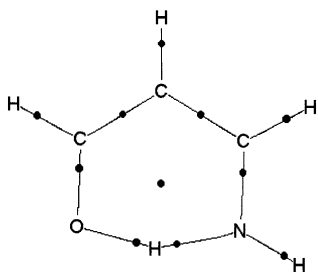


Figure 7. Molecular graph of one of the TSs investigated here; circles correspond to BCPs and RCP.

nitrogen atom participating within the H-bond strongly influences the type of tautomer; for the strongly electronegative F substituent, the tautomeric form containing the O—H \cdots N bond is energetically favorable while for the Li substituent at the same position only a tautomer with a N—H \cdots O bond exists. Such a situation is observed for the crystal structures investigated here since the only differences within molecular structures concern the R₄ substituents (Scheme 2) attached to the mentioned above nitrogen atom. This substituent is N(CH₃)—P(O)(OC₆H₅)₂ for **1** and NH—P(S)(OC₆H₅)₂ for **2**. It seems that the first one is more electronegative than the second one (oxygen atom and sulfur atom attached to the phosphorus atom for **1** and **2**, respectively). It is in line with the other crystal structures of phosphorochromones investigated earlier^{12–14} since for the species with intramolecular H-bonds only the N—H \cdots O systems exist and there are sulfur atoms connected with phosphorus atoms for them.

Acknowledgment. This work was financially supported by the University of Łódź (Grant No. 505/667 2001) and the State Committee for Scientific Research, Grant No. 3 T09A 061 19 (S.J.G.). S.J.G. wishes to acknowledge the Interdisciplinary Center for Mathematical and Computational Modeling (Warsaw University) for computational facilities. Financial support for J.N.-M. from the Medical University of Łódź (Grant No. 502-13-850 202) is gratefully acknowledged.

Supporting Information Available: CIF files for the mentioned structures. This material is available free of charge via the Internet at <http://pubs.acs.org>.

References and Notes

- Gabor, M. *The Pharmacology of Benzopyrane Derivatives and Related Compounds*; Akadémiai Kiadó: Budapest, 1988.
- Harborne, J. B. *The Flavonoids Advances In Research Since 1986*; Chapman Hall: London, 1994.
- Valentini, P.; Fabbri, G.; Rampa, A.; Bisi, A.; Gobbi, S.; Da Re, P.; Carrara, M.; Sgevano, A.; Cima, L. *Anti-Cancer Drug Des.* **1996**, *11*, 243.
- Mouysset, G.; Bellan, J.; Payard, M.; Tisne-Versailles, J. *Farmaco Ed. Sci.* **1987**, *42*, 805.
- Arnold, H.; Bourseaux, F.; Brock, N. *Nature* **1958**, *181*, 931.
- Meyers, F. H.; Jawetz, E.; Goldfein, A. *Review of Medical Pharmacology*, 5th ed.; Lange Medical Publications: Los Atlos, 1976.
- Schroeder, D. C.; Corcoran, P. O.; Holden, C. L.; Mulligan, M. A. *J. Org. Chem.* **1961**, *27*, 1098.
- Cates, L. A.; Lemke, T. L. *J. Pharm. Sci.* **1974**, *63*, 1736.
- Nawrot-Modranka, J.; Kostka, K. *Pol. J. Chem.* **1995**, *69*, 1148.
- Nawrot-Modranka, J.; Kostka, K. *Pol. J. Chem.* **1995**, *69*, 1250.
- Preussmann, R.; Schneider, H.; Epple, F. *Arzneim. Forsh.* **1969**, *19*, 1059.
- Rybarczyk, A. J.; Olszak, T. A.; Malecka, M.; Nawrot-Modranka, J. *Acta Crystallogr. Sect. C* **1999**, *55*, 1313.
- Rybarczyk-Pirek, A. J.; Zgierski, M. Z. *J. Chem. Phys.* **2001**, *115*, 9346.
- Rybarczyk, A. J.; Malecka, M.; Grabowski, S. J.; Nawrot-Modranka, J. *Acta Crystallogr. Sect. C* **2002**, *58*, o405.
- Ellis, G. P. *The Chemistry of Heterocyclic Compounds. Chromenes, Chromanones and Chromones*; John Wiley and Sons Inc.: New York, 1977; pp 488–489.
- Cambridge Structural Database System; Cambridge Crystallographic Data Centre: Cambridge, U.K., 2001.
- (a) Gilli, G.; Belluci, F.; Ferretti, V.; Bertolasi, V. *J. Am. Chem. Soc.* **1989**, *111*, 1023. (b) Gilli, P.; Bertolasi, V.; Ferretti, V.; Gilli, G. *J. Am. Chem. Soc.* **1994**, *116*, 909. (c) Bertolasi, V.; Gilli, P.; Ferretti, V.; Gilli, G. *Acta Crystallogr.* **1995**, *B51*, 1004.
- Bader, R. F. W. *Atoms in Molecules. A Quantum Theory*; Oxford University Press: New York, 1990.
- MSC/AFC Diffractometer Control Software; Molecular Structure Corporation: The Woodlands, U.S.A., 1989.
- Kuma KM4 Diffractometer Software; Kuma Diffraction: Wroclaw, Poland, 1996.
- de Meulenaer, J.; Tompa, H. *Acta Crystallogr. Sect. A* **1965**, *19*, 1014.
- Farrugia, L. J. *J. Appl. Crystallogr.* **1999**, *32*, 837.
- Sheldrick, G. M. *SHELXS86 Program for Crystal Structure Solution*; University of Göttingen: Germany, 1986.
- Sheldrick, G. M. *SHELX97 Programs for Crystal Structure Analysis*; University of Göttingen: Germany, 1997.
- Nardelli, M. *J. Appl. Crystallogr.* **1996**, *29*, 296.
- Spek, A. L. *PLATON—Molecular Geometry Program*; University of Utrecht: The Netherlands, 1998.
- Frisch, M. J.; Trucks, G. W.; Schlegel, H. B.; Gill, P. M. W.; Johnson, G. B.; Robb, M. A.; Cheeseman, J. R.; Keith, T. A.; Petersson, G. A.; Montgomery, J. A.; Raghavachari, K.; Al-Laham, M. A.; Zakrzewski, V. G.; Ortiz, J. V.; Foresman, J. B.; Cioslowski, J.; Stefanov, B. B.; Nanayakkara, A.; Challacombe, M.; Peng, C. Y.; Ayala, P. Y.; Chen, W.; Wong, M. W.; Andres, J. L.; Replogle, E. S.; Gomperts, R.; Martin, L. R.; Fox, D. J.; Binkley, J. S.; Defrees, D. J.; Steward, J. J.; Head-Gordon, M.; Gonzalez, G.; Pople, J. A. *Gaussian 94*; Gaussian, Inc.: Pittsburgh, PA, 1995.
- Frisch, M. J.; Trucks, G. W.; Schlegel, H. B.; Scuseria, G. E.; Robb, M. A.; Cheeseman, J. R.; Zakrzewski, V. G.; Montgomery, J. A.; Stratmann, R. E.; Burant, J. C.; Dapprich, S.; Millam, J. M.; Daniels, A. D.; Kudin, K. N.; Strain, M. C.; Farkas, O.; Tomasi, J.; Barone, V.; Cossi, M.; Cammi, R.; Mennucci, B.; Pomelli, C.; Adamo, C.; Clifford, S.; Ochterski, J.; Petersson, G. A.; Ayala, P. Y.; Cui, Q.; Morokuma, K.; Malick, D. K.; Rabuck, A. D.; Raghavachari, K.; Foresman, J. B.; Cioslowski, J.; Ortiz, J. V.; Stefanov, B. B.; Liu, G.; Liashenko, A.; Piskorz, P.; Komaromi, I.; Gomperts, R.; Martin, L. R.; Fox, D. J.; Keith, T.; Al-Laham, M. A.; Peng, C. Y.; Nanayakkara, A.; Gonzalez, G.; Challacombe, M.; Gill, P. M. W.; Johnson, B.; Chen, W.; Wong, M. W.; Andres, J. L.; Gonzalez, C.; Head-Gordon, M.; Replogle, E. S.; Pople, J. A. *Gaussian 98*; Revision A.6; Gaussian, Inc.: Pittsburgh, PA, 1998.
- Møller, C.; Plesset, M. S. *Phys. Rev.* **1934**, *46*, 618.
- Scheiner, S. *Hydrogen Bonding: A Theoretical Perspective*; Oxford University Press: New York, 1997.
- Koch, U.; Popelier, P. *J. Phys. Chem.* **1995**, *99*, 9747.
- Fuster, F.; Silvi, B. *Theor. Chem. Acc.* **2000**, *104*, 13.
- Etter, M. C.; MacDonald, J. C.; Bernstein, J. *Acta Crystallogr. Sect. B* **1990**, *46*, 256.
- Allen, F. H.; Kennard, O.; Watson, D. G.; Brammer, J. L.; Orpen, A. G.; Taylor, R. *J. Chem. Soc., Perkin. Trans. 2* **1987**, S1–S19.
- Scheiner, S.; Kar, T.; Čuma, M. *J. Phys. Chem. A* **1997**, *101*, 5901.
- Kar, T.; Scheiner, S.; Čuma, M. *J. Chem. Phys.* **1999**, *111*, 849.
- González, L.; Mó, O.; Yáñez, M. *J. Phys. Chem. A* **1997**, *101*, 9710.
- González, L.; Mó, O.; Yáñez, M. *J. Org. Chem.* **1999**, *64*, 2314.
- Grabowski, S. J. *J. Mol. Struct.* **2001**, *562*, 137.
- Rovira, M. C.; Scheiner, S. *J. Phys. Chem.* **1995**, *99*, 9854.
- Bertolasi, V.; Gilli, P.; Ferretti, V.; Gilli, G. *Acta Crystallogr.* **1994**, *B50*, 617.
- Bürgi, H. B. *Angew. Chem., Int. Ed. Engl.* **1975**, *14*, 460.
- Dunitz, J. D. *X-ray Analysis and the Structure of Organic Molecules*; Cornell University Press: Ithaca and London, 1979.
- Grabowski, S. J.; Krygowski, T. M. *Chem. Phys. Lett.* **1999**, *305*, 247.
- Grabowski, S. J.; Krygowski, T. M.; Stępień, B. *J. Phys. Org. Chem.* **2000**, *13*, 740.
- Carrol, M. T.; Chang, C.; Bader, R. F. W. *Mol. Phys.* **1988**, *63*, 387.
- Carrol, M. T.; Bader, R. F. W. *Mol. Phys.* **1988**, *65*, 695.
- Espinosa, E.; Souhassou, M.; Lachekar, H.; Lecomte, C. *Acta Crystallogr.* **1999**, *B55*, 563.
- Grabowski, S. J. *J. Phys. Chem. A* **2000**, *104*, 5551.
- Grabowski, S. J. *Chem. Phys. Lett.* **2001**, *338*, 361.
- Grabowski, S. J. Horizons in H-bond Research, Proceeding of the Conference, Torino, September, 2001.
- Popelier, P. *Atoms in Molecules, An Introduction*; Prentice Hall, Pearson Education Limited: New York, 2000.